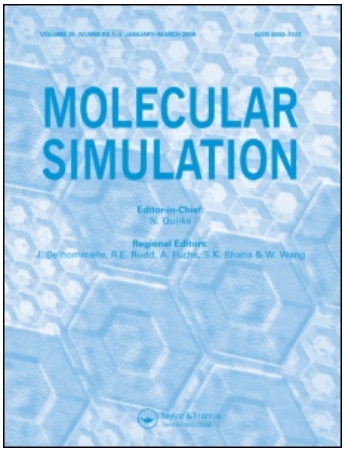


## Molecular Simulation

Publication details, including instructions for authors and subscription information:
http://www.informaworld.com/smpp/title~content=t713644482

# Local Behavior of Water Molecules on Brucite, Talc, and Halite Surfaces: A Molecular Dynamics Study

Hiroshi Sakuma[a]; Taku Tsuchiya[b]; Katsuyuki Kawamura[c]; Kenshiro Otsuki[a]

[a] Institute of Geology and Paleontology, Graduate School of Science, Tohoku University, Sendai, Japan [b] Department of Chemical Engineering and Materials Science (CEMS), Minnesota University, Minneapolis, MN, USA [c] Department of Earth and Planetary Sciences, Tokyo Institute of Technology, Tokyo, Japan

**To cite this Article** Sakuma, Hiroshi , Tsuchiya, Taku , Kawamura, Katsuyuki and Otsuki, Kenshiro(2004) 'Local Behavior of Water Molecules on Brucite, Talc, and Halite Surfaces: A Molecular Dynamics Study', Molecular Simulation, 30: 13, 861 — 871

**To link to this Article: DOI:** 10.1080/08927020412331299350

**URL:** http://dx.doi.org/10.1080/08927020412331299350

*Molecular Simulation*, VOL. 30 (13–15), 15 November–30 December 2004, pp. 861–871

Taylor & Francis
Taylor & Francis Group

# Local Behavior of Water Molecules on Brucite, Talc, and Halite Surfaces: A Molecular Dynamics Study

HIROSHI SAKUMA[a,*], TAKU TSUCHIYA[b], KATSUYUKI KAWAMURA[c] and KENSHIRO OTSUKI[a]

[a]*Institute of Geology and Paleontology, Graduate School of Science, Tohoku University, Aoba, Aramaki, Aoba-ku, Sendai 9808578, Japan;*
[b]*Department of Chemical Engineering and Materials Science (CEMS), Minnesota University, 421 Washington Av. SE, Minneapolis, MN 55455, USA;*
[c]*Department of Earth and Planetary Sciences, Tokyo Institute of Technology, 2-12-1 Ookayama, Meguro-ku, Tokyo 1528551, Japan*

*(Received January 2004; In final form August 2004)*



**The structural and dynamic properties of water between brucite (0001), talc (001), and halite (100) surfaces have been calculated by classical molecular dynamics (MD) simulations at ambient conditions. The interaction potential models between water and the minerals have been developed by the energy curves obtained from the *ab initio* electronic state calculations. Orientational anisotropy of water molecules is almost limited in the vicinity of all the surfaces. The significant different properties of water between the surfaces are observed in the density profiles and self-diffusion coefficients. The density profile of water between talc surfaces is flat and the density is equivalent to the bulk one, while those of water between brucite and halite surfaces strongly oscillate with the distance from the surfaces. The self-diffusion coefficients parallel to the surfaces are enhanced in the vicinity of brucite and talc surfaces, and reduced on halite surface compared with that in bulk.**

*Keywords*: Surface diffusion; Water; Solid–liquid interfaces; Anisotropy

## INTRODUCTION

Water plays a significant role in various important areas such as biochemistry, chemistry, physics and earth science. In particular, the effect of water is evident in the phenomena occurring at the interfaces of solid surfaces [1–3]. The structural and dynamic properties of water at or near surfaces are different from the properties in the bulk state [1,2] and the detail properties of adsorbed and interlayer water between various solid surfaces are extremely important to be revealed.

The density profiles and orientation of water molecules on solid surfaces have been experimentally investigated. The high-resolution specular X-ray reflectivity has revealed that the density of water oxygen on muscovite (001) oscillates to the surface-normal direction, giving evidence of interfacial water ordering [4]. There are several experimental techniques for evaluating the orientation of water on solid surfaces such as work function change (e.g. Ref. [5]), electron-stimulated desorption, ion angular detection (ESDIAD) [6], and near-edge X-ray absorption fine structure (NEXAFS) [7]. These have indicated that the preferable orientations of water molecules on some solid surfaces ($TiO_2$, Ru, and Ni) are with oxygen-end down and one or both O—H bonds oriented away from the surface.

The dynamic property of adsorbed water would be understood from the translational and rotational motions of water molecules. The self-diffusion coefficients ($D_S$) and reorientation times ($\tau_{NMR}$) are useful for investigating the dynamic property of water. In our knowledge, there is no research for the rotational motion of water molecules on solid surfaces. The self-diffusion of adsorbed water has been one of the difficult properties investigated by experimental study [2]. *Ab initio* and classical molecular dynamics (MD) simulations are one of the most useful tools to investigate not only density profiles and orientation but also self-diffusion coefficients of water. These computer simulations have great advantage for the detail analysis of water behavior compared with experiments. For example, the self-diffusion coefficients of water can be obtained with the distance from the surfaces [8]. An ice-like structure of water molecules at monolayer coverage on muscovite (001) even at 300 K has been reported by *ab initio* MD simulations [9].

*Corresponding author. Address: Institute of Multidisciplinary Research for Advanced Materials, Tohoku University, 2-1-1 Katahira, Aoba-ku, Sendai 9808577, Japan. E-mail: hsaku@tagen.tohoku.ac.jp

ISSN 0892-7022 print/ISSN 1029-0435 online © 2004 Taylor & Francis Ltd
DOI: 10.1080/08927020412331299350

Large self-diffusion coefficient on brucite (0001) has been observed by classical MD simulations using *ab initio* fitted model potential [8]. These phenomena may be due to the characteristic interaction between water molecules and the mineral surfaces. However, the systematic understanding of water behavior on various surfaces is insufficient yet.

Here, we review the previous researches for three mineral surfaces (brucite, talc, and halite). Brucite ($Mg(OH)_2$) has the basic structure with stacking of trioctahedral sheets of the edge-sharing $MgO_6$ octahedra and hydroxyl. Since it is a typical layer mineral having hydroxyl groups on the (0001) cleavage surface, it is suitable to study the water behavior on the surface having hydroxyl groups. Related with brucite, MgO–water system has been investigated by *ab initio* MD [10,11], classical MD [12], and experimental approaches [13–16]. The *ab initio* MD indicated that an $H_2O$ molecule in the proximity of a perfect (001) surface is physisorbed. On the other hand, for a stepped surface, the dissociation of water molecules proceeds. The experimental works found that highly defective MgO crystal changed its surface to that of brucite ($Mg(OH)_2$) by contact with water by using atomic force microscope (AFM), synchrotron-based photoemission spectroscopy (PES), low-energy electron diffraction, and X-ray standing wave (XSW) techniques. After full hydroxylation, additional water can be physisorbed on the hydroxylated MgO surface, which is almost equivalent to a brucite (0001) surface. Talc ($Mg_3Si_4O_{10}(OH)_2$) is a trioctahedral 2:1 clay mineral whose surface consists of rings of $SiO_4$ tetrahedra. Hydroxyl groups belonging to the octahedral sheet lie at the centers of these rings. The oxygen atoms are exposed at the (001) cleavage surface and measurement of contact angle of water on talc indicates that a freshly cleaved surface is hydrophobic [17]. Therefore it is suitable to study the water behavior on hydrophobic surfaces. Talc–water system has been investigated by Monte Carlo simulation [18]. However, the interaction between water molecules and talc surface was not rigorously determined. So it is difficult to discuss the physical properties of water on talc from this simulation. Halite (NaCl) is a typical ionic crystal showing the strong electrolytic character in water and it is significant to compare with brucite and talc. On the (100) surface arrays of Na and Cl ions form the face-centered square 2D lattice. Thus, though there is no distinct electric moment normal to the surface as well as talc, the large field gradient exists parallel to the surface. Favorable adsorption geometries of water on a clean NaCl (100) surface have been reported by the *ab initio* calculations [19]. They also found that the water–water interaction becomes dominant for more than monolayer adsorption, and ice-like structure can be easily destroyed with increasing temperature.

Classical MD simulations were used in this study to obtain the enough ensemble averages for calculating self-diffusion coefficients and reorientation times. The massive computational resources needed to the *ab initio* calculations limit the system size and the time range, while classical MD realizes the large system size and long time calculations. In order to obtain the reliable results by classical MD simulations, the interaction between water and mineral surfaces should be determined properly. As performed by our previous works [8], we made and used the *ab initio* fitted model potential between water and mineral surfaces.

In this work, we present the MD simulations of water behavior embedded between brucite (0001), talc (001), and halite (100) and compare the effect of the surfaces on water behavior. The structural property of water is discussed from the density profiles and orientational statistics and the dynamic property of water is discussed from the self-diffusion coefficients and reorientation times.

## MINERAL AND WATER MODELS

In this study, the interatomic potential function was used. The two-body part is described as follows:

$$\begin{aligned} U_{ij}(r_{ij}) = {} & \frac{1}{4\pi\varepsilon_0}\frac{z_i z_j e^2}{r_{ij}} + f_0(b_i+b_j)\exp\left[\frac{a_i+a_j-r_{ij}}{b_i+b_j}\right] \\ & - \frac{c_i c_j}{r_{ij}^6} + D_{1ij}\Big\{\exp\left[-2\beta_{1ij}(r_{ij}-r_{1ij})\right] \\ & - 2\exp\left[-\beta_{1ij}(r_{ij}-r_{1ij})\right]\Big\} \\ & + D_{3ij}\exp\left[-\beta_{3ij}(r_{ij}-r_{3ij})^2\right], \end{aligned}$$

where the first term denotes the Coulomb interaction between $i$ and $j$ atom, the second term the short-range repulsion, the third term the van der Waals interaction, the fourth and fifth term the radial covalent bond. The parameters in these terms, $\varepsilon_0$ is the dielectric constant of vacuum, $z_i$ the partial charge of atom $i$, $e$ the elementary charge, $r_{ij}$ the distance between the atoms $i$ and $j$, $f_0$ the constant for the converting unit [$= 41.8605\,\mathrm{kJ/(nm\,mol)}$], $a_i$ the repulsion diameter, $b_i$ the softness coefficient, $c_i$ the van der Waals coefficient for atoms. $D_{1ij}$, $\beta_{1ij}$, $r_{1ij}$, $D_{3ij}$, $\beta_{3ij}$, and $r_{3ij}$ are used of atom pairs for the adjustment of the radial covalent bonds.

The three-body part is described as follows:

$$\begin{aligned} U_{ijk}(\theta_{ijk}, r_{ij}, r_{jk}) &= -f\{\cos[2(\theta_{ijk}-\theta_0)]-1\}\times(k_1\times k_2)^{1/2}, \\ k_1 &= \frac{1}{\exp[g_r(r_{ij}-r_m)]+1}, \\ k_2 &= \frac{1}{\exp[g_r(r_{jk}-r_m)]+1}. \end{aligned}$$

The parameters in these terms, $\theta_{ijk}$ denotes the angle between atoms $i$–$j$–$k$. $\theta_0$, $f$, $g_r$, and $r_m$ are

TABLE I Potential parameters of brucite, talc, halite, and water models. Coulomb, short-range repulsion and van der Waals terms. The '–' denotes that the parameter is not used.

| *No.* | *Atom* | *z (e)* | *Weight (g/mol)* | *a (nm)* | *b (nm)* | *c (kJ/mol)$^{1/2}$(nm)$^3$* |
|---|---|---|---|---|---|---|
| (a) Brucite | | | | | | |
| 1 | O | −1.180 | 16.00 | 0.1870 | 0.0167 | 0.047058 |
| 2 | Mg | 1.500 | 24.31 | 0.0974 | 0.0053 | 0.006138 |
| 3 | H | 0.430 | 1.01 | 0.0044 | 0.0044 | – |
| (b) Talc | | | | | | |
| 4 | O | −1.280 | 16.00 | 0.1863 | 0.0160 | 0.018414 |
| 5 | Si | 2.500 | 28.09 | 0.0940 | 0.0080 | – |
| 6 | Mg | 1.500 | 24.31 | 0.0960 | 0.0067 | 0.006138 |
| 7 | H | 0.430 | 1.01 | 0.0044 | 0.0046 | – |
| (c) Halite | | | | | | |
| 8 | Cl | −1.000 | 35.45 | 0.2109 | 0.0210 | 0.068745 |
| 9 | Na | 1.000 | 22.99 | 0.1431 | 0.0100 | 0.012481 |
| (d) Water | | | | | | |
| 10 | O | −0.9172 | 16.00 | 0.1728 | 0.01275 | 0.056060 |
| 11 | H | 0.4586 | 1.010 | 0.0035 | 0.0044 | – |

Two body terms for covalent bond

| *Atom (no.)–atom (no.)* | *$D_{1ij}$ (kJ/mol)* | *$\beta_{1ij}$ (nm$^{-1}$)* | *$r_{1ij}$ (nm)* | *$D_{3ij}$ (kJ/mol)* | *$\beta_{3ij}$ (nm$^{-2}$)* | *$r_{3ij}$ (nm)* |
|---|---|---|---|---|---|---|
| O(1)–H(3) | 96.70 | 29.80 | 0.1070 | 31.81 | 1180.00 | 0.1328 |
| O(4)–Si(5) | 131.02 | 20.00 | 0.1500 | – | – | – |
| O(4)–H(7) | 59.44 | 32.00 | 0.1117 | 31.81 | 1180.00 | 0.1328 |
| O(10)–H(11) | 54.84 | 31.80 | 0.0980 | 34.74 | 1280.00 | 0.1283 |

Three body terms for covalent bond

| *Atom–atom–atom* | *f (kJ)* | *$\theta_0$ (degree)* | *$r_m$ (nm)* | *$g_r$ (nm$^{-1}$)* |
|---|---|---|---|---|
| H(3)–O(1)–H(3) | $1.16\times10^{-22}$ | 99.50 | 0.1480 | 92.0 |
| H(7)–O(4)–H(7) | $1.16\times10^{-22}$ | 99.50 | 0.1480 | 92.0 |
| H(11)–O(10)–H(11) | $1.15\times10^{-22}$ | 99.50 | 0.1430 | 92.0 |



the adjustment parameters for the angular part of covalent bonds.

The potential parameters of atoms of minerals were empirically determined to reproduce the physical properties in bulk state such as lattice constants (brucite model, $a = 3.142$ Å, $c = 4.760$ Å, $V = 40.69$ Å$^3$; talc model, $a = 5.259$ Å, $b = 9.124$ Å, $c = 19.021$ Å, $\beta = 96.62°$, $V = 906.64$ Å$^3$; halite model, $a = 5.638$ Å, $V_0 = 179.26$ Å$^3$ at ambient conditions), structure, elasticity (brucite model, $K_0 = 41.40$ GPa, $K_0' = 7.64$; talc model, $K_0 = 42.78$ GPa, $K_0' = 10.31$; halite model, $K_0 = 24.63$ GPa, $K_0' = 4.78$), and vibrational spectra. The potential parameters of atoms of water molecule were also empirically determined to reproduce the densities ($\rho$), static dielectric constants ($\varepsilon$), self-diffusion coefficients ($D_S$), reorientation times ($\tau_{NMR}$), and vibrational spectra over the wide range of temperature and pressure conditions. These values at 298.15 K and 0.1 MPa are as follows: $\rho = 0.9958 \pm 0.0029$ g/cm$^3$, $\varepsilon = 70.04 \pm 1.28$, $D_S = (1.475 \pm 0.008)\times10^{-9}$ m$^2$/s, $\tau_{NMR} = 3.346 \pm 0.161$ ps. This water model tends to give small self-diffusion coefficients and large reorientation times compared with experimental values [20,21]. However, this flexible water model is one of the best water models among the rigid, flexible and polarizable models to reproduce the physical properties of water and ice over the wide range of temperature and pressure conditions. The potential parameters are shown in Table I.

## INTERACTION BETWEEN WATER AND MINERAL SURFACES

The first step in performing the simulations of mineral–water interfaces is to develop a reliable and consistent model for the interaction of water molecules with solid surfaces [22]. Fundamental understanding of such interactions often requires physico-chemical knowledge at the molecular level, which is not easily obtained from experimental works. Electronic state calculations can provide remarkable information of the interactions between surface species and water molecules [23–25]. The first-principles method based on the density functional theory is the most useful method in the present day. It is also highly adaptable for the hydrogen bonding systems as shown in many previous studies [26–29].

The geometrical optimization of a water molecule on the brucite, talc, and halite surfaces was performed to find the stable configurations. After that the energy changes were calculated as a function of distance from the surface by shifting the position of the water molecule. To solve electronic structure, we employed plane-wave basis and pseudopotential method with

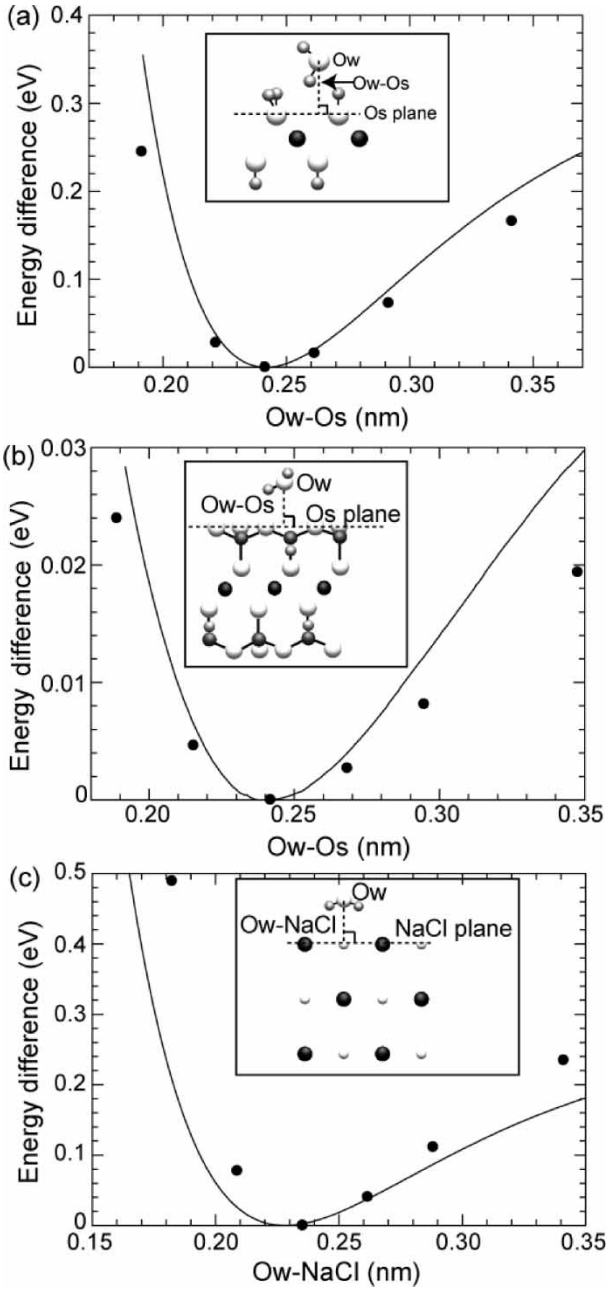


FIGURE 1 Potential energy curves between a water molecule and (a) brucite, (b) talc, and (c) halite surfaces. The solid line and solid circles denote the results of the model and *ab initio* calculations, respectively. The insets show the snapshots of most stable structure of an isolated $H_2O$ on each surface calculated by *ab initio* calculations.

the gradient correction [30] for the exchange and correlation energy. Pseudopotentials were made by the Troullier–Martins method [31]. The energy cut-off of the plane-wave basis was set to be 60 hartree, which is enough to converge the total energy within $0.1 \times 10^{-3}$ hartree. The detailed calculation methods and results are shown in the paper [32].

We constructed the *ab initio* fitted model potentials interacting between a water molecule and brucite, talc, and halite surfaces using the energy-distance data. The potential energy curves used for fitting the parameter are shown in Fig. 1. The equilibrium distance of oxygen of a water molecule from the surfaces is almost same between models and *ab initio* calculations. It should be noted from the *ab initio* calculations that the adsorption energy on talc surface is much smaller than those on brucite and halite surfaces. As shown in inset figures, a water molecule on each surface has different orientation at the most stable configuration. Since halite is considered as a typical ionic crystal, the covalent bond interaction between water molecules and halite surfaces would be small. Therefore, the covalent terms of interatomic potential function between halite and water molecules are not used in this study. The potential parameters fitted to the *ab initio* data are shown in Table II.

## COMPUTATIONAL METHODS

Classical MD simulations were performed by MXDORTO [33]. For calculating the Coulomb interactions, the Ewald sum method was applied. Differential equation of motion of atoms was converted to the difference equation of the velocity Verlet algorithm. Time increment for the difference equation is 0.4 fs. The ensemble averages were taken from 200 ps runs. The unit cell is of rectangular parallelepiped. The MD calculations were carried out with NPT ensemble ($P = 0.1$ MPa, $T = 298.15$ K). To maintain the constant "$P$" pressure condition, we controlled the stress elements of a unit cell. The off-diagonal element cannot be controlled in the rectangular parallelepiped cell, but the shear elements were relaxed due to the existence of liquid water in the equilibrium state. In this way, the constant "$P$" pressure control was carried out. Our reported error bars represent 90 percent standard deviation error estimates from the 3 separate runs.

The snapshots are shown in Fig. 2a–c. The 300 $H_2O$ molecules and a mineral structure with surfaces (360 $Mg(OH)_2$ or 72 $Mg_3Si_4O_{10}(OH)_2$ or 576 NaCl) were contained in a unit cell of three-dimensional periodic boundary conditions for each system. The side lengths of the unit cell are $3.14 \times 3.26 \times 2.44$ nm in brucite–water, $2.73 \times 3.16 \times 3.32$ nm in talc–water, and $3.36 \times 3.36 \times 3.12$ nm in halite–water system at each equilibrium state. The 2.44, 3.32, and 3.12 nm correspond to the length perpendicular to the brucite (0001), talc (001), and halite (100) surfaces, respectively, and the others correspond to the lengths parallel to the surfaces.

## RESULTS AND DISCUSSION

### Orientation

Orientational statistics is one of the important factors to know the bonding geometry between

TABLE II Potential parameters of *ab initio* fitted model

| Two body terms for covalent bond | | | | | | |
|---|---|---|---|---|---|---|
| *Atom (no.)–atom (no.)* | $D_{1ij}$ *(kJ/mol)* | $\beta_{1ij}$ $(nm^{-1})$ | $r_{1ij}$ *(nm)* | $D_{3ij}$ *(kJ/mol)* | $\beta_{3ij}$ $(nm^{-2})$ | $r_{3ij}$ *(nm)* |
| O(1)–H(11) | 4.19 | 40.00 | 0.0940 | 34.74 | 1280.00 | 0.1000 |
| H(3)–O(10) | 104.65 | 44.00 | 0.1000 | 34.74 | 1280.00 | 0.1283 |
| O(4)–H(11) | 1.67 | 31.80 | 0.0980 | 34.74 | 1280.00 | 0.1283 |
| Si(5)–O(10) | 79.53 | 23.00 | 0.1500 | – | – | – |
| H(7)–O(10) | 54.84 | 31.80 | 0.0980 | 34.74 | 1280.00 | 0.1283 |
| Three body terms for covalent bond | | | | | | |
| *Atom–atom–atom* | *f (kJ)* | $\theta_0$ *(degree)* | $r_m$ *(nm)* | $g_r$ $(nm^{-1})$ | | |
| H(11)–O(1)–H(11) | $1.15 \times 10^{-22}$ | 99.50 | 0.1430 | 92.0 | | |
| H(11)–O(4)–H(11) | $1.15 \times 10^{-22}$ | 99.50 | 0.1430 | 92.0 | | |
| H(3)–O(10)–H(3) | $1.15 \times 10^{-22}$ | 99.50 | 0.1430 | 92.0 | | |
| H(7)–O(10)–H(7) | $1.15 \times 10^{-22}$ | 99.50 | 0.1430 | 92.0 | | |

Coulomb, short-range repulsion and van der Waals terms of atoms and the other covalent terms of atom pairs are same as shown in Table I.

water molecules and mineral surfaces. MD simulations can easily investigate the orientation of adsorbed water molecules on solid surfaces. Probability densities of orientational statistics are shown in Fig. 3. The definition of orientation of a water molecule is shown in Fig. 3a. Since the orientational anisotropy of water molecules would be changed with the distances from the surfaces, it was investigated for the layers having 0.25 nm thickness in the direction. The layer numbers shown in Fig. 3 correspond to the numbers described in Fig. 2. The layer 1 is the nearest layer



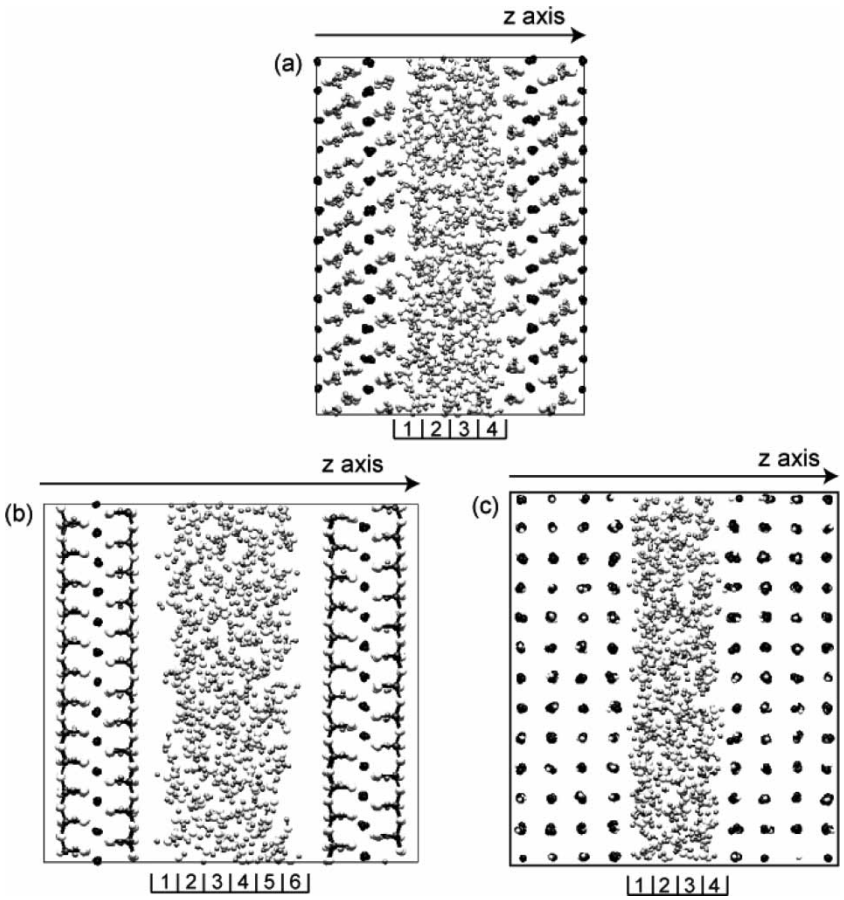


FIGURE 2 Snapshots of unit cells of (a) brucite–water, (b) talc–water, and (c) halite–water system at 298.15 K and 0.1 MPa. In (a), the black, light gray, white spheres denote the magnesium, hydrogen, and oxygen atoms, respectively. In (b), black, light gray, dark gray, and white spheres denote the magnesium, hydrogen, silicon, and oxygen atoms, respectively. In (c), black, small white, large white, and light gray spheres denote the chlorine, sodium, oxygen, and hydrogen atoms, respectively. The *z*-axes denote the perpendicular direction to the brucite (0001), talc (001), and halite (100). The lower numbers denote the numbers of sliced layers having *ca.* 2.5 Å thickness.

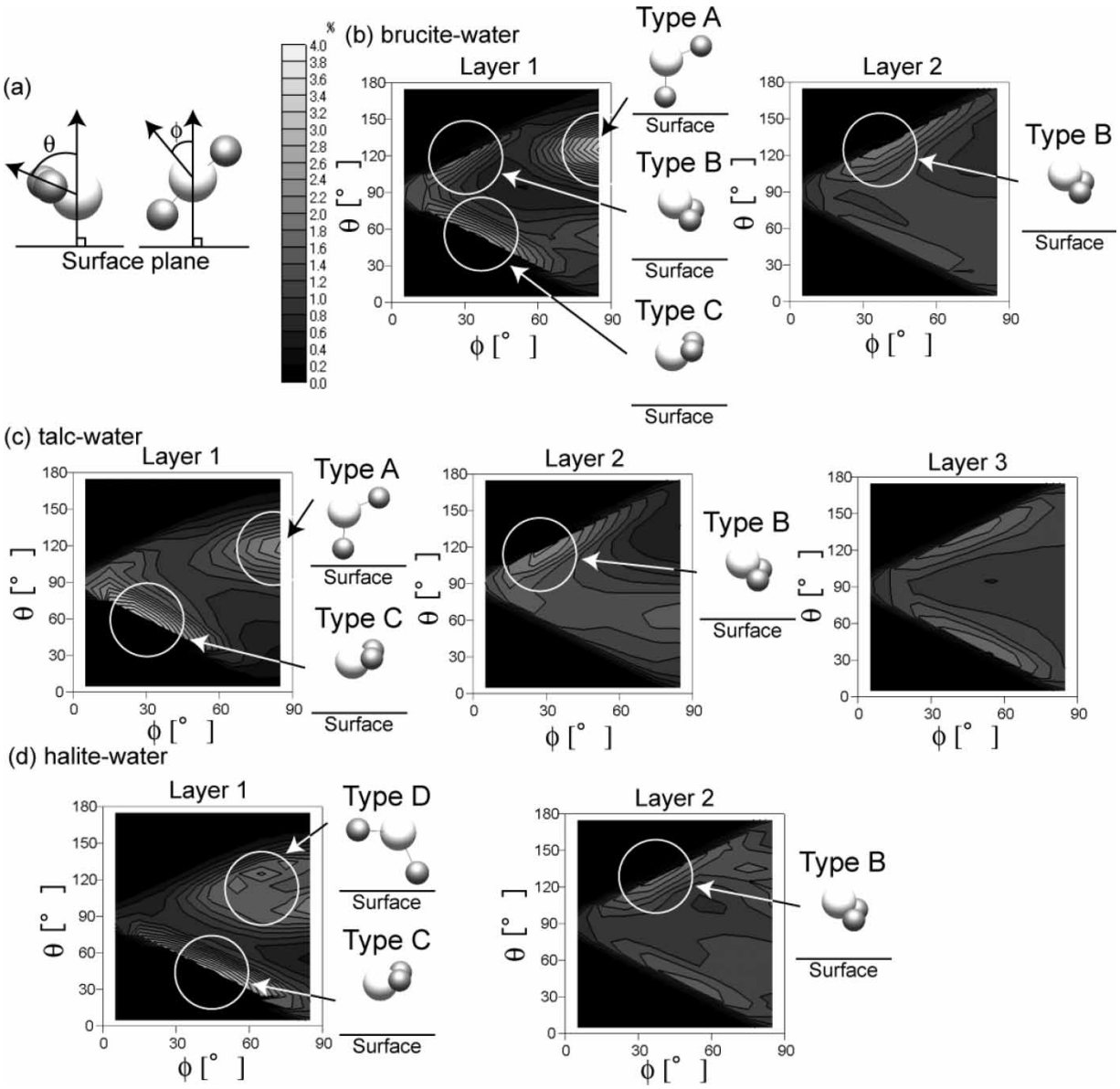


FIGURE 3 Orientational statistics of water molecules between (b) brucite, (c) talc, and (d) halite surfaces. Orientation of water molecules was defined by two angles, $\theta$ and $\phi$ (a). The $\theta$ is the angle between dipole moment vector and normal vector of the surface. The $\phi$ is the angle between the outer product vector of O—H vectors and the normal vector of the surface. The layer number indicates the area shown as the lower number of snapshots in Fig. 2.

to the surfaces, and the layers 2 and 3 are 0.25 and 0.5 nm further layers from the surfaces, respectively. Since the orientational statistics is almost symmetric about the centers, the left-hand sides of unit cell shown in the snapshots (Fig. 2) are discussed here.

The anisotropy of orientation near brucite surface is noticeable at layer 1 and slightly distinguishable at layer 2 (Fig. 3b). It indicates that the effect of brucite surface on the orientation is almost limited in layer 1. There are three dominant orientational types (A, B and C) at layer 1 and type B slightly appears at layer 2. The type A molecule is similar to the most stable structure calculated by structure optimization of a water molecule on brucite (0001) (see Fig. 1). The population having type A configuration is large mainly in the layer 1, type B molecules are found both in the layers 1 and 2, and the population having the type C configuration decreases with separation from the surface. The type A and type C molecules make hydrogen bonds with surface oxygen and hydrogen, respectively. The type B molecules make hydrogen bonds with the type A and type C molecules.

The anisotropy of orientation near talc surface is also noticeable at layer 1 and slightly distinguishable at layer 2 (Fig. 3c). The significant difference from that of brucite surface is that the type B molecules cannot be seen at layer 1. There are two dominant orientational types (A and C) at layers 1 and in particular the type C has large population.

The population having type A configuration is large mainly in layer 1 and the population having type C configuration decreases with the distance from the surface. In the layer 2, the type B has large population. It indicates that the type A molecules adsorb on talc surface by making the weak hydrogen bonding with oxygen atoms of the surface. The type B molecules make hydrogen bonding with the type A and type C molecules. The type C molecules make hydrogen bonding with the type A and type B molecules.

The anisotropy of orientation near halite surface is also noticeable at layer 1 and slightly distinguishable at layer 2 (Fig. 3d). This trend is in common with water molecules on brucite and talc surfaces. There are two dominant orientational types (C and D) at layer 1. The type D has large population mainly at layer 1 and the population having type C configuration decreases with the distance from the surface. In the layer 2, type B has slightly large population. It indicates that the type D molecules adsorb on halite surface by making attractive interaction between hydrogen atoms of water molecules and chloride ions of the surface. The type B molecules make hydrogen bonding with the type C and type D molecules. The type C molecules make attractive interaction between oxygen atoms of water molecules and sodium ions of the surface.

The orientational statistics revealed that two or three types of orientations have large population in the vicinity of the surfaces and these orientational anisotropies are almost limited in the vicinity of the surfaces.

### Density Profiles

Density profiles have been considered as an indicator of the structuring of water [34,35]. Density profiles of water molecules between mineral surfaces are shown in Fig. 4. The thickness of water thin film estimated from the widths of density profiles between brucite, talc, and halite surfaces are 0.85, 1.30, and 0.75 nm, respectively. Since the profiles are almost symmetric about the centers, the left hand sides are discussed here.

Density profile of water between brucite surfaces is shown in Fig. 4a. The first peak is at 0.87 nm and having the shoulder at 0.96 nm. Note that these distances indicate the position along with the *z*-axis shown in Fig. 2. These densities of first peak and shoulder have 1.9 times and 1.1 times higher than in bulk water, respectively. The density of second maximum at 1.22 nm is 1.4 times as high as in bulk water. Compared with the discussion of orientation, the first peak and the shoulder would correspond to the type A and C water molecules, respectively. The second peak exists just in the center of the water film. Thus, both the solid surfaces equally affect the water orientation. Therefore, water cannot have specific orientation and the second peak may be strongly affected by this system size. There is no significant density oscillation between talc surfaces (Fig. 4b). The density profile is almost flat and the density is same as bulk water. The orientational anisotropy is not related to the density oscillation. Density profile of water between halite surfaces is shown in Fig. 4c. The density of first peak at 1.19 nm has 2.4 times as high as in bulk water and the second small peak is at 1.39 nm. The height of first peak is higher than the peak between brucite surfaces. Compared with the discussion of orientation, the first peak corresponds to the type C and D molecules and the second peak to the type B molecules.

The density oscillation of water molecules on mineral surfaces would be related to the adsorption energy of the surfaces. The large adsorption energy attracts the water molecules strongly to the surfaces and the density of water molecules becomes high in

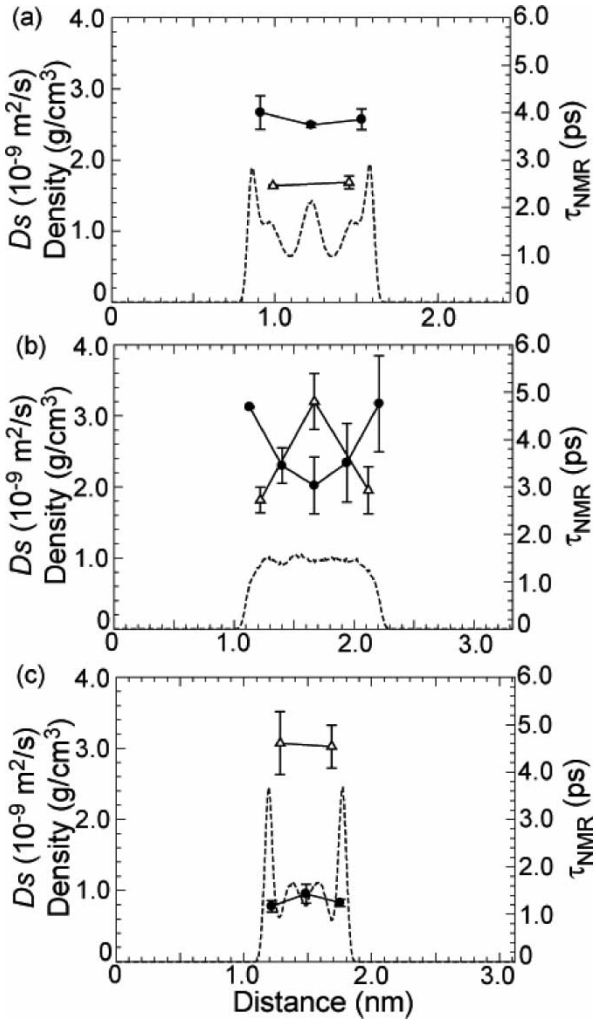


FIGURE 4 Density profiles (broken lines), self-diffusion coefficients, $D_S$ (solid circles), and reorientation times, $\tau_{NMR}$ (triangles) of water between (a) brucite, (b) talc, and (c) halite surfaces. The abscissa axes denote the distance along with the *z*-axes shown in Fig. 2a–c.

the vicinity of the surfaces. The adsorption energy of the surfaces can be estimated from the depth of the potential energy curves between a water molecule and the surfaces (Fig. 1). The estimated adsorption energies of brucite, talc, and halite surfaces are 0.26, 0.04, and 0.36 eV, respectively [32]. These adsorption energies are well agreement with the degree of oscillation of density profile on each surface. On the halite surface, the adsorption energy is high and the density profile strongly oscillates. On the other hand, on the talc surface, the adsorption energy is low and the density profile becomes flat.

It is known that the density oscillation diminishes with the distance from a mineral surface [4,24] and the decay length indicates the surface effect on the structure of water. Obviously, the effect of talc is small, however, the comparison of the effect among brucite and halite cannot be discussed in this study, because of the short surface separations of brucite and halite. It should be investigated in the larger system.

### Self-diffusion Coefficients ($D_S$) and Reorientation Times ($\tau_{NMR}$)

$D_S$ were calculated from the velocity auto-correlation function [36] and the $D_S$ can be expressed as follows.

$$D_S = \frac{1}{d}\int_0^\infty \mathrm{VACF}(t)\mathrm{d}t.$$

In this equation, $d$ denotes the dimensionality of the system and $\mathrm{VACF}(t) = \langle \mathbf{v}(t) \times \mathbf{v}(0) \rangle$ is the ensemble average of the velocity auto-correlation function. To obtain the proper self-diffusion coefficients of bulk water at ambient conditions, it needs integrated time period from 0 to 1.0 ps [37]. The time period was taken from 0 to 1.5 ps. The $D_S$ in this study denotes the self-diffusion coefficients of water molecules parallel to the mineral surfaces and calculated from the two-dimensional velocity auto-correlation function. To obtain the local self-diffusion coefficients of water, $D_S$ were calculated at each sliced layer having 0.25 nm thickness along with normal to the surfaces.

$\tau_{NMR}$ were calculated from $C_2^y(t)$ shown as

$$C_2^y(t) = \frac{1}{2}\left\langle 3\{\mathbf{e}(t)\cdot\mathbf{e}(0)\}^2 - 1\right\rangle.$$

The **e** denotes the vector connecting the hydrogen atoms of a water molecule. The zero frequency component of the Fourier transform of $C_2^y(t)$ gives the NMR relaxation time $\tau_{NMR}$. The correlation function, $C_2^y(t)$, can be approximated by a long-range exponential decay, $A_2^y \exp(-t/\tau_2^y)$, and a short-range oscillatory part. The zero frequency part of the Fourier transform of $C_2^y(t)$ is, to a good approximation, given by $A_2^y\tau_2^y$, because the short-range part will not contribute much to the Fourier transform [38]. To obtain the local $\tau_{NMR}$ of water, $\tau_{NMR}$ were calculated at each sliced layer having 0.5 nm thickness along with the normal to the surfaces.

Calculated $D_S$ and $\tau_{NMR}$ are shown in Fig. 4a–c. The $D_S$ of water between brucite surfaces (Fig. 4a) show higher values compared with that in the bulk. It indicates that water molecules confined between brucite surfaces can move 1.7–1.8 times faster than in bulk. The $\tau_{NMR}$ of water between brucite surfaces has 0.76 times longer than that of bulk water and it indicates that water molecules can rotate faster than in the bulk water. The $D_S$ and $\tau_{NMR}$ between talc surfaces are shown in Fig. 4b. It is found that the $D_S$ of water in the vicinity of talc surface is 2.1 times higher than in the bulk and the $D_S$ decreases with the distance from the talc surface. The $\tau_{NMR}$ of water in the vicinity of talc surfaces has 0.9 times longer than that of bulk water and it indicates that water molecules can rotate faster than in the bulk water. In the middle layer, the $\tau_{NMR}$ of water molecules has 1.5 times longer than that in bulk water. The $D_S$ and $\tau_{NMR}$ between halite surfaces are shown in Fig. 4c. The $D_S$ of water between halite surfaces shows the lower values compared with in the bulk and in particular in the vicinity of surfaces. The $D_S$ in the vicinity of halite surface is half value of bulk water. The $\tau_{NMR}$ of water between halite surfaces has the high values and it corresponds to 1.4 times longer than in the bulk water.

The potential barrier between stable sites can give some insights to these different behaviors of $D_S$ in the vicinity of three different mineral surfaces. In order to move parallel to the surface, water molecules must cross over the potential barrier between stable sites [24]. The contour maps of potential energy surface (Fig. 5) give us the indication of translational motion of water molecules on the mineral surfaces. The contour maps were obtained as follows. The water molecule at most stable state on the surface was moved parallel to the surface with the orientation of the water molecule fixed, and the potential energy was calculated at each configuration. The effect of neighboring water molecules is not considered in these maps. Considering with water molecules moving parallel to the surfaces, water molecules must cross over the potential barrier of 0.3, 0.3, and 0.6 eV for brucite, talc, and halite surfaces, respectively. The actual potential barrier would be smaller than these estimated values, since the potential barrier was calculated with fixed the orientation of the water molecule. The potential barriers of brucite and talc are low and therefore water molecules can move easily. On the other hand, that of halite is high and therefore water molecules cannot move easily.

The $D_S$ of water between talc surfaces decreases with the distance from surface, but those of water between brucite and halite surfaces do not show such change. Additional simulations with larger

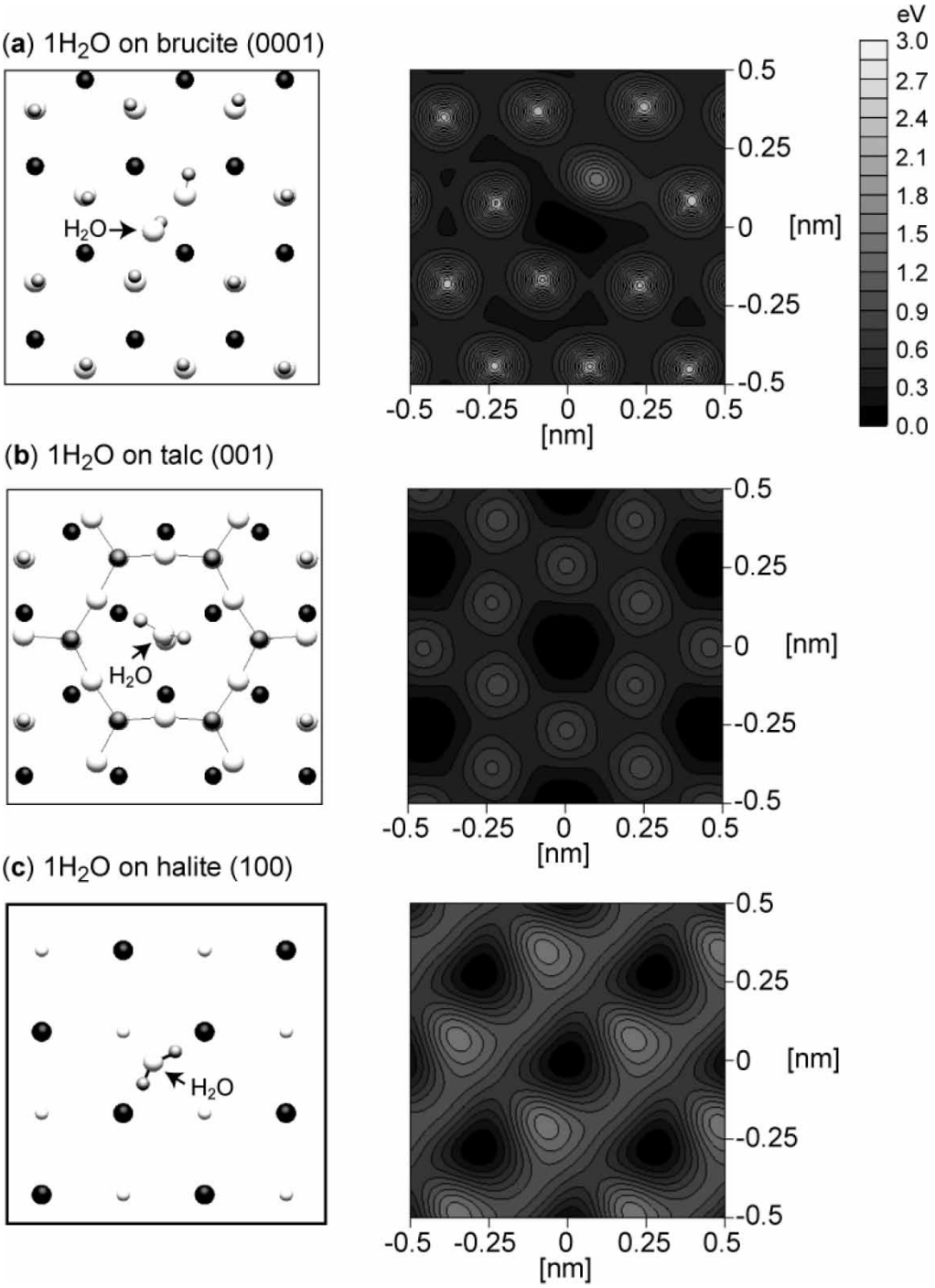


FIGURE 5 Snapshots of most stable configuration (left hand side) and contour maps of potential energy surface (right hand side) for a water molecule on (a) brucite (0001), (b) talc (001), and (c) halite (100) surfaces. These contour maps were calculated by using the model interaction.

separations should be performed to reveal this difference between brucite, talc, and halite.

The reason of the change of $\tau_{NMR}$ might be understood from the number of intermolecular bonds of the water molecules. Since the water molecule making many intermolecular bonds needs much energy to break the bonds to rotate, a water molecule cannot easily rotate. Therefore the number of intermolecular bonds in the vicinity of brucite and talc surfaces might be less than that in the bulk water and the number in the vicinity of halite might be more than that in the bulk water.

## CONCLUSIONS

To study the water behavior by classical MD simulations, *ab initio* potential energy surface was

used to fit parameters of interatomic potential models of water with brucite (0001), talc (001), and halite (100) surfaces. We calculated the structural (molecular orientation and density profiles) and dynamic (self-diffusion and reorientation times) properties of water molecules between brucite (0001), talc (001), and halite (100) at 298.15 K and 0.1 MPa. The molecular orientational anisotropy is almost limited in the vicinity of the surfaces. Density of water between talc surfaces is flat and equivalent to the bulk value, but those of water between brucite and halite surfaces strongly oscillate with the distance from the surfaces. This difference can be understood from the adsorption energy of a water molecule to the surfaces. Self-diffusion coefficients parallel to the surfaces are large in the vicinity of brucite and talc surfaces, and small in the vicinity of halite surface. This difference is generated from the potential energy barrier of surfaces to travel between stable sites for a water molecule. Brucite and talc has low and halite has high potential barrier. The reorientation times in the vicinity of brucite and talc surfaces are long and that in the vicinity of halite surface is short. This difference may be explained from the number of interatomic bonds of water molecules.

These simulations have shown that water molecules in the interface region have different structural and dynamic properties due to the species of solid surfaces.



## *Acknowledgements*

This research was partially supported by the Ministry of Education, Science, Sports and Culture, Grant-in-Aid for Exploratory Research, 14654076, 2002–2003.

## *References*

[1] Thiel, P.A. and Madey, T.E. (1987) "The interaction of water with solid surfaces: fundamental aspects", *Surf. Sci. Rep.* **7**, 211.
[2] Henderson, M.A. (2002) "The interaction of water with solid surfaces: fundamental aspects revisited", *Surf. Sci. Rep.* **46**, 1.
[3] Morrow, C.A., Moore, D.E. and Lockner, D.A. (2000) "The effect of mineral bond strength and adsorbed water on fault gouge frictional strength", *Geophys. Res. Lett.* **27**, 815.
[4] Cheng, L., Fenter, P., Nagy, K.L., Schlegel, M.L. and Sturchio, N.C. (2001) "Molecular-scale density oscillations in water adjacent to a mica surface", *Phys. Rev. Lett.* **87**, 156103.
[5] Hugenschmidt, M.B., Gamble, L. and Campbell, C.T. (1994) "The interaction of $H_2O$ with a $TiO_2$(110) surface", *Surf. Sci.* **302**, 329.
[6] Madey, T.E. and Yates, J.T., Jr. (1977) "Evidence for the conformation of $H_2O$ adsorbed on Ru(001)", *Chem. Phys. Lett.* **51**, 77.
[7] Pangher, N., Schmalz, A. and Haase, J. (1994) "Structure determination of water chemisorbed on Ni(110) by use of X-ray absorption fine-structure measurements", *Chem. Phys. Lett.* **221**, 189.
[8] Sakuma, H., Tsuchiya, T., Kawamura, K. and Otsuki, K. (2003) "Large self-diffusion of water on brucite surface by *ab initio* potential energy surface and molecular dynamics simulations", *Surf. Sci.* **536**, L396.
[9] Odelius, M., Bernasconi, M. and Parrinello, M. (1997) "Two-dimensional ice adsorbed on mica surface", *Phys. Rev. Lett.* **78**, 2855.
[10] Langel, W. and Parrinello, M. (1994) "Hydrolysis at stepped MgO surfaces", *Phys. Rev. Lett.* **73**, 504.
[11] Langel, W. and Parrinello, M. (1995) "*Ab initio* molecular dynamics of $H_2O$ adsorbed on solid MgO", *J. Chem. Phys.* **103**, 3240.
[12] de Leeuw, N.H. and Parker, S.C. (1998) "Molecular-dynamics simulation of MgO surfaces in liquid water using a shell-model potential for water", *Phys. Rev. B* **58**, 13901.
[13] Mejias, J.A., Berry, A.J., Refson, K. and Fraser, D.G. (1999) "The kinetics and mechanism of MgO dissolution", *Chem. Phys. Lett.* **314**, 558.
[14] Liu, P., Kendelewicz, T., Brown, G.E., Jr. and Parks, G.A. (1998) "Reaction of water with MgO(100) surfaces. Part I: Synchrotron X-ray photoemission studies of low-defect surfaces", *Surf. Sci.* **412/413**, 287.
[15] Liu, P., Kendelewicz, T. and Brown, G.E., Jr. (1998) "Reaction of water with MgO (100) surfaces. Part II: Synchrotron photoemission studies of defective surfaces", *Surf. Sci.* **412/413**, 315.
[16] Liu, P., Kendelewicz, T., Nelson, E.J. and Brown, G.E., Jr. (1998) "Reaction of water with MgO(100) surfaces. Part III: X-ray standing wave studies", *Surf. Sci.* **415**, 156.
[17] Schrader, M.E. and Yariv, S. (1990) "Wettability of clay minerals", *J. Colloid Interface Sci.* **136**, 85.
[18] Bridgeman, C.H. and Skipper, N.T. (1997) "A Monte Carlo study of water at an uncharged clay surface", *J. Phys.: Condens. Matter* **9**, 4081.
[19] Meyer, H., Entel, P. and Hafner, J. (2001) "Physisorption of water on salt surfaces", *Surf. Sci.* **488**, 177.
[20] Krynicki, K., Green, C.D. and Sawyer, D.W. (1978) "Pressure and temperature dependence of self-diffusion in water", *Faraday Discuss. Chem. Soc.* **66**, 199.
[21] Jonas, J., DeFries, T. and Wilbur, D.J. (1976) "Molecular motions in compressed liquid water", *J. Chem. Phys.* **65**, 582.
[22] Parker, S.C., de Leeuw, N.H., Bourova, E. and Cooke, D.J. (2001) "Application of lattice dynamics and molecular dynamics techniques to minerals and their surfaces", *Rev. Mineral. Geochem.* **42**, 63.
[23] Chacon-Taylor, M.R. and McCarthy, M.I. (1996) "*Ab initio* based classical electrostatic potentials for the interaction between molecules and surfaces", *J. Phys. Chem.* **100**, 7610.
[24] McCarthy, M.I., Schenter, G.K., Scamehorn, C.A. and Nicholas, J.B. (1996) "Structure and dynamics of the water/MgO interface", *J. Phys. Chem.* **100**, 16989.
[25] Bussai, C., Hannongbua, S., Fritzsche, S. and Haberlandt, R. (2002) "*Ab initio* potential energy surface and molecular dynamics simulations for the determination of the diffusion coefficient of water in silicalite-1", *Chem. Phys. Lett.* **354**, 310.
[26] Benoit, M., Marx, D. and Parrinello, M. (1998) "Tunnelling and zero-point motion in high-pressure ice", *Nature* **392**, 258.
[27] Ramaniah, L.M., Bernasconi, M. and Parrinello, M. (1999) "*Ab initio* molecular-dynamics simulation of $K^+$ solvation in water", *J. Chem. Phys.* **111**, 1587.
[28] Silvestrelli, P.L. and Parrinello, M. (1999) "Water molecule dipole in the gas and in the liquid phase", *Phys. Rev. Lett.* **82**, 3308.
[29] Sprik, M., Hutter, J. and Parrinello, M. (1996) "*Ab initio* molecular dynamics simulation of liquid water: comparison of three gradient-corrected density functionals", *J. Chem. Phys.* **105**, 1142.

[30] Perdew, J.P., Burke, K. and Ernzerhof, M. (1996) "Generalized gradient approximation made simple", *Phys. Rev. Lett.* **77**, 3865.
[31] Troullier, N. and Martins, J.L. (1991) "Efficient pseudo-potentials for plane-wave calculations", *Phys. Rev. B* **43**, 1993.
[32] Tsuchiya, T., Sakuma, H. and Tsuchiya, J. (2004) "*Ab initio* investigation of water, aqueous solution and water–solid interface", In: Nakashima, S, ed., *Physicochemistry of Water and Dynamics of Materials and the Earth* (Universal Academy Press, Inc.), pp 59–86.
[33] Kawamura, K. (1996) Society of Computer Chemistry, Japan, www.sccj.net/, #29.
[34] Fenter, P., Geissbühler, P., DiMasi, E., Srajer, G., Sorensen, L.B. and Sturchio, N.C. (2000) "Surface speciation of calcite observed *in situ* by high-resolution X-ray reflectivity", *Geochim. Cosmochim. Acta* **64**, 1221.
[35] Fenter, P., McBride, M.T., Srajer, G., Sturchio, N.C. and Bosbach, D. (2001) "Structure of barite (001)- and (210)-water interfaces", *J. Phys. Chem. B* **105**, 8112.
[36] Frankel, D. and Smit, B. (2002) *Understanding Molecular Simulation. From Algorithms to Applications*, 2nd Ed. (Academic Press).
[37] Nymand, T.M. and Linse, P. (2000) "Molecular dynamics simulations of polarizable water at different boundary conditions", *J. Chem. Phys.* **112**, 6386.
[38] Impey, R.W., Madden, P.A. and McDonald, I.R. (1982) "Spectroscopic and transport properties of water model calculations and the interpretation of experimental results", *Mol. Phys.* **46**, 513.